

## 1

## Biosensing using Carbon Nanotube Field-effect Transistors

*Padmakar D. Kichambare and Alexander Star*

## 1.1

### Overview

This chapter covers recent advances in biodetection using single-walled carbon nanotube field-effect transistors (NTFETs). In particular, we describe fabrication of NTFET devices and their application for electronic detection of biomolecules. A typical NTFET fabrication process consists of combination of chemical vapor deposition (CVD) and complementary metal oxide semiconductor (CMOS) processes. The NTFET devices have electronic properties comparable to traditional metal oxide semiconductor field-effect transistors (MOSFETs) and readily respond to changes in the chemical environment, enabling a direct and reliable pathway for detection of biomolecules with extreme sensitivity and selectivity. We address the challenges in effective integration of carbon nanotubes into conventional electronics for biosensor applications. We also discuss in detail recent applications of NTFETs for label-free electronic detection of antibody–antigen interactions, DNA hybridization, and enzymatic reactions.

## 1.2

### Introduction

The interplay between nanomaterials and biological systems forms an emerging research field of broad importance. In particular, novel biosensors based on nanomaterials have received considerable attention [1–4]. Integration of one-dimensional (1D) nanomaterials, such as nanowires, into electric devices offers substantial advantages for the detection of biological species and has significant advantages over the conventional optical biodetection methods [5]. The first advantage is related to size compatibility: Electronic circuits in which the component parts are comparable in size to biological entities ensure appropriate size compatibility between the detector and the detected biological species. The second advantage to developing nanomaterial based electronic detection is that most biological processes involve electrostatic interactions and charge transfer, which are directly

detected by electronic nanocircuits. Nanowire-based electronic devices, therefore, eventually integrate the biology and electronics into a common platform suitable for electronic control and biological sensing as well as bioelectronically driven nanoassembly [6].

One promising approach for the direct electrical detection of biomolecules uses nanowires configured as field-effect transistors (FETs). FETs readily change their conductance upon binding of charged target biomolecules to their receptor linked to the device surfaces. For example, recent studies by Lieber's group have demonstrated the use of silicon nanowire FETs for detecting proteins [7], DNA hybrids [8], and viruses [9]. This biodetection approach may allow in principle selective detection at a single particle levels [10, 11]. Nanowires hold the possibility of very high sensitivity detection owing to the depletion or accumulation of charge carriers, which are caused by binding of a charged biomolecules at the surface. This surface binding can affect the entire cross-sectional conduction pathway of these nanostructures. For some nanowires, such as hollow carbon nanotubes, every atom is on the surface and exposed to the environment; even small changes in the charge environment can drastically change their electrical properties. Thus, among different nanomaterials, carbon nanotubes have a great potential for biosensing.

Among numerous applications of carbon nanotubes [12–14], carbon nanotube based sensing technology is rapidly emerging into an independent research field. As for any new research field, there is no yet consensus in the literature about the exact sensing mechanism. In this chapter, in addition to selected examples of carbon nanotube based sensors, we address the controversial carbon nanotube sensing mechanism.

To date, sensor applications of carbon nanotubes have been summarized and discussed in several excellent review articles [15–17], which primarily focus on carbon nanotube based electrochemical sensors. This chapter covers only recent advances in biodetection using carbon nanotube field-effect transistors (NTFETs). It is divided into two large sections: NTFET fabrication and their sensor applications. Section 1.3 gives a detailed description of NTFET device structure, its fabrication method and introduces device characteristics. This section also addresses technical challenges in effective integration of carbon nanotubes into CMOS electronics. Section 1.4, which focuses on sensor applications of NTFETs, is divided into several subsections. Before discussing NTFET application for biological detection we describe the effect of environmental conditions on NTFET device characteristics. We give selected examples of NTFET sensitivity for small molecules, mobile ions, and water (relative humidity). The effect of these factors should be well understood before NTFET biodetection is reviewed. We also briefly describe the operation of NTFETs in conducting media, which is particularly important for biosensor applications. Then we briefly summarize interactions of carbon nanotubes with biomolecules (e.g., polysaccharides, DNA and proteins) to set a stage for the subsequent subsections that describe in great details recent applications of NTFETs for label-free electronic detection of proteins, antibody–antigen interactions, DNA hybridization, and enzymatic reactions.

### 1.3

## Carbon Nanotube Field-effect Transistors (NTFETs)

### 1.3.1

#### Carbon Nanotubes

Since their discovery by Iijima over a decade ago [18], interest in carbon nanotubes has grown considerably [19]. Recent advances in the synthesis and purification of carbon nanotubes have turned them into commercially available materials. Subsequently, several experiments have been undertaken to study the physical and electrical properties of carbon nanotubes on the individual and macroscopic scale [20–23]. On the macroscopic scale, spectroscopic and optical absorption measurements have been carried out to test the purity of the carbon nanotubes [24, 25]. For electronic transport measurements it is particularly interesting to perform experiments on isolated, individual carbon nanotubes. The properties of carbon nanotubes depend strongly on physical aspects such as their diameter, length, and presence of residual catalyst [12]. The properties measured from a large quantity of nanotubes could be an average of all nanotubes in the sample, so that the unique characteristics of individual carbon nanotubes could be shadowed. Experiments on individual nanotubes are very challenging due to their small size, which prohibits the application of well-established testing techniques. Moreover, their small size also makes their manipulation rather difficult. Specialized techniques are needed to mount or grow an individual carbon nanotube on the electrode with sub-micron precision.

Carbon nanotubes are hollow cylinders made of sheets of carbon atoms and can be divided into single-walled carbon nanotubes (SWNTs) and multi-walled carbon nanotubes (MWNTs). SWNTs possess a cylindrical nanostructure with a high aspect ratio, formed by rolling up a single graphite sheet into a tube (Fig. 1.1). SWNTs are, typically, a few nanometers in diameter and up to several microns long. MWNTs consist of several layers of graphene cylinders that are concentrically nested like rings of a tree trunk, with an interlayer spacing of  $3.4 \text{ \AA}$  [26]. Because of their unique properties, carbon nanotubes have become a material that has generated substantial interest on nanoelectronic devices and nanosensors [27, 28]. These properties are largely dependent upon physical aspects such as diameter, length, presence of catalyst and chirality. For example, SWNT can be metallic or semiconducting, depending upon the intrinsic band gap and helicity [29]. Semiconducting SWNTs can be used to fabricate FET devices, as demonstrated by Dekker and co-workers [30]. In addition, semiconducting SWNTs exhibit significant conductance changes in response to the physisorption of different gases [24, 31, 32]. Therefore, SWNT-based nanosensors can be fabricated based on FET layout, where the solid-state gate is replaced by adsorbed molecules that modulate the nanotube conductance [33]. Since semiconducting SWNTs have a very high mobility and, because all their atoms are located at the surface, they are the perfect nanomaterial for sensors. These sensors offer several advantages for the detection of biological species. First, carbon nanotubes form the conducting channel in a transistor configura-

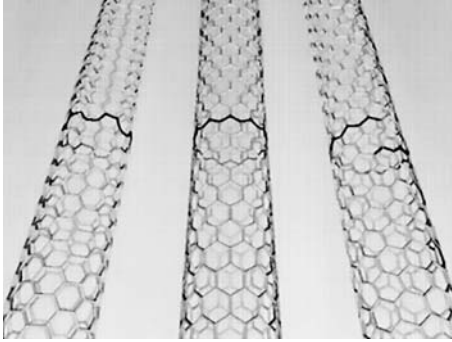


**Fig. 1.1.** A seamlessly rolled-up single graphite sheet forms a single-walled carbon nanotube (SWNT). SWNTs are, typically, a few nanometers in diameter and up to several micrometers long. They can be either metallic

or semiconducting, depending on their helicity and diameter. Semiconducting SWNTs are used for the fabrication of nanotube field-effect transistors (NTFETs). (Adapted with permission from Ref. [4], © Wiley-VCH Verlag).

tion. Second, the nanotubes are typically located on the surface of the supporting substrate and are in direct contact with the environment. This device geometry contrasts with traditional metal oxide semiconductor field-effect transistors (MOSFETs) where the conducting channel is buried in the bulk material in which the depletion layer is formed. Lastly, all of the electrical current flows at the surface of nanotubes. All these remarkable characteristics lead to a FET device configuration that is extremely sensitive to minute variations in the surrounding environment.

### 1.3.2

#### Nanotube Synthesis

Several synthesis methods are used to produce carbon nanotubes [34]. The three most commonly used methods are the arc discharge, laser ablation, and chemical vapor deposition (CVD) techniques. While the arc and laser methods can produce large quantities of carbon nanotubes they lead to resilient contaminants, including pyrolytic and amorphous carbon [35, 36], which are difficult to remove from the sample. Such impurities result in low recovery yield for the carbon nanotube product. However, recent advances in scaling up these methods, as well as development new fabrication methods such as high pressure carbon monoxide (HiPCO), have created commercial supplies of carbon nanotubes with more than 90% purity with competitive prices. In contrast, the less scalable CVD process offers the best chance of obtaining controllable routes for the selective production of carbon nanotubes with defined properties [37]. CVD is catalytically driven, wherein a metal catalyst is used in conjunction with the thermal decomposition of hydrocarbon feedstock gases to produce carbon nanotubes. In most cases, the resultant growth of nanotubes occurs on a fixed substrate within the process. Figure 1.2 illustrates a typical CVD process for the generation of SWNTs. SWNTs are synthesized by the

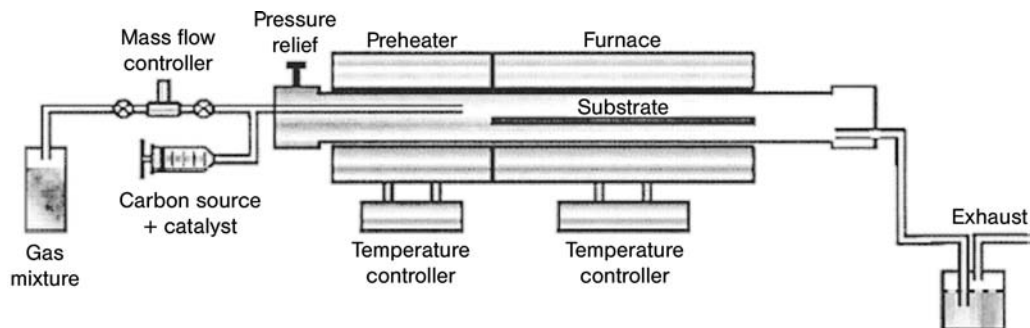


**Fig. 1.2.** Schematic of a chemical vapor deposition (CVD) reactor that uses a two-zone furnace. Carbon nanotubes grow on the substrate placed inside the quartz tube. (Reprinted with permission from Ref. [34], © 2001, CRC Press).

reaction of a hydrocarbon (e.g.,  $\text{CH}_4$ ) vapor over a dispersed Fe catalyst. The synthesis apparatus consists of a quartz tube reactor inside a combined preheater and furnace set-up. The preheat section is operated at  $\sim 200^\circ\text{C}$ . The catalysts are deposited and then hydrocarbon vapors are carried into the reaction zone of the furnace. An Ar/(10%)- $\text{H}_2$  carrier gas is used that controls the partial pressure inside the quartz tube reactor. Reaction temperatures are typically in the range  $900\text{--}1000^\circ\text{C}$ . The SWNTs grow on the substrates (Fig. 1.3) and form thick mats that are readily harvested. This process produces highly pure SWNTs at a yield approaching 50% conversion of all hydrocarbon feedstock into carbon nanotube product. Similarly, a CVD processes sometimes utilize a feed of hydrocarbon-catalyst liquid for the production of nanotubes, and for this purpose a syringe pump is used to allow the continuous injection of this solution into a preheat section. Various gaseous feed-stocks are used to produce nanotubes, ranging from  $\text{CH}_4$  to  $\text{C}_2\text{H}_2$ . A wide range of transition metals and rare earth promoters have been investigated for the synthesis of SWNTs by CVD. In general, a transition metal is the major component in the catalyst particles used regardless of the catalyst support. The most common metals found to be successful in the growth of SWNTs are Fe, Co, and Ni [38, 39]. However, bimetallic catalysts consisting of Fe/Ni, Co/Ni, or Co/Pt [40] are re-

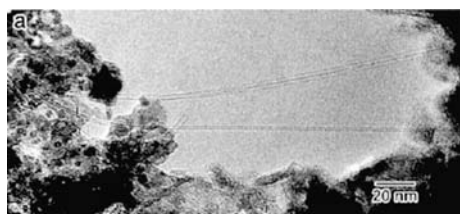


**Fig. 1.3.** Transmission electron microscopy (TEM) image of an SWNT synthesized by chemical vapor deposition (CVD). (Reprinted with permission from Ref. [37], © 2001, The American Chemical Society).

ported to give the best yield of nanotubes, in addition to some rare earth metals that have also been studied [41].

Despite challenges, the understanding the growth mechanism of SWNTs is crucial for, ultimately, tailoring the production of SWNTs with known lengths, diameters, helical structures and placement of SWNTs at the desired location. Presently, efforts are underway to understand the mechanism of catalytic growth of SWNTs on surfaces and the role of impurities and to increase nanotube yield by varying the substrate, catalyst, and growth conditions [42]. Directional growth of SWNTs has been achieved by electric fields [43, 44], gas flow [45], lattice directions [46], and atomic steps [47].

### 1.3.3

#### Fabrication of NTFETs

To date carbon nanotubes have been used to fabricate various devices, including nanotube-based mechanical devices [48] and field emission devices [13]. This section focuses specifically on fabrication of carbon nanotube field-effect transistors (NTFETs). Figure 1.4(a) shows a schematic drawing of NTFET. A semiconducting carbon nanotube is contacted by source and drain electrodes while the gate elec-

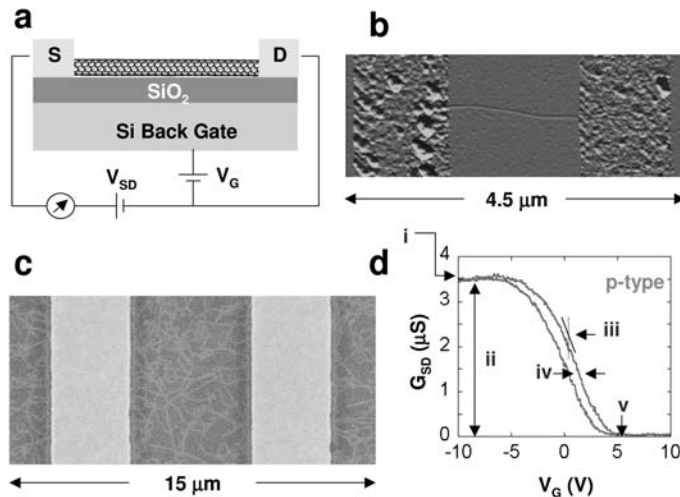


**Fig. 1.4.** (a) Schematic representation of a nanotube field-effect transistor (NTFET) device with a semiconducting SWNT contacted by two Ti/Au electrodes, representing the source (S) and the drain (D) with a Si back gate separated by a SiO<sub>2</sub> insulating layer in a transistor-configured circuit. (b) Atomic force microscopy (AFM) image of a typical NTFET device consisting of a single semiconducting

SWNT. (c) Scanning electron microscopy (SEM) image of a typical NTFET device consisting of a random array of carbon nanotubes. (d) Typical NTFET transfer characteristic – dependence of the source-drain conductance ( $G_{SD}$ ) on the gate voltage ( $V_G$ ) – (i) maximum conductance, (ii) modulation, (iii) transconductance, (iv) hysteresis, and (v) threshold voltage.

trode, which is electrically insulated from the nanotube channel, is used to manipulate the nanotube's conductivity. Depending on the particular method of nanotube fabrication, a NTFET can be structured in different ways [49]. However, most publications on nanotube transistors report the use of a degenerately doped Si-substrate with a comparatively thick (100–500 nm) thermally grown oxide layer [30, 50–53]. Silicon substrates are readily available and can be used with both bulk-produced nanotubes and nanotubes grown directly on the Si-substrate by CVD. If doped highly, the Si substrate stays conductive even at low temperatures, making it usable as a so-called back-gate with the  $\text{SiO}_2$  as a stable, if low- $k$ , gate dielectric. Bulk produced nanotubes (laser ablation [54] or HiPCO [55]) are usually purified and deposited onto Si substrates by suspending them in organic solvents (e.g., chloroform, dichloroethane, etc.) and then spin-coating or drop casting on the substrates. In this approach the nanotubes create a random network over the substrate surface. Alignment of the nanotubes is possible, if an AC dielectric field is applied during deposition [56]. Generally, two different configurations of NTFETs, regarding source and drain contacts, are possible. By patterning the contacts before nanotube deposition [30] one can contact nanotubes in bulk, whereas by depositing the contacts onto the nanotubes one contacts only the ends of nanotubes [57], because depositing contact material on top of the nanotube normally destroys the nanotubes underneath the contacts. The second configuration usually guarantees a lower contact resistance than what is achievable in bulk-contacted devices [58]. Room temperature NTFET manufacturing methods, while compatible with CMOS, are limited by ability to disperse effectively carbon nanotubes in the solution and deposit them without further aggregation on device surfaces [59]. Nanotube bundle formation may decrease the semiconducting character of NTFET due to the occasional presence of nanotube bundles containing metallic nanotubes.

For CVD grown carbon nanotubes metal contacts are deposited onto the nanotubes [60, 61], because typical contact materials cannot withstand CVD temperatures, thus making it impossible to grow carbon nanotubes on CMOS structures. Often, the metal contacts are annealed to lower contact resistance [62]. Several studies have tried to optimize the material used for the contacts, including Cr/Au [49] and Pt [30], but only the Cr/Au contacts have been used widely. In this type of contact the chromium layer is a thin (1–3 nm) adhesion layer that facilitates adhesion of the gold to  $\text{SiO}_2$ . An adhesion layer of Ti [63], especially when annealed, allows deposition of smooth films of many metals onto carbon nanotubes because Ti forms titanium carbide at the interface with the nanotube. For this reason, Ti/Au-contacts are another frequently used combination of contact materials. Many publications investigating Schottky barriers between a nanotube and its contacts [61, 64] have employed such contacts. Palladium (Pd) is another material investigated that wets nanotubes well and has been used recently to produce NTFETs with ohmic contacts, i.e., contacts without Schottky barriers [52, 63].

Depending on the number of carbon nanotubes connecting the source and drain electrodes, there are two different device architectures. In the first device architecture, a single nanotube connects the source and drain (Fig. 1.4b). These devices have been used for biosensing with excellent sensitivity. However, there is substan-

tial variation between the different devices that are fabricated and this variation is reflected in the electronic characteristics of individual nanotubes. In addition, the interface between the nanotube and the metallic contact may vary from device to device. Specialized techniques are needed either to mount or grow an individual carbon nanotube at a predetermined location. Placement is difficult and impractical for mass fabrication of NTFETs. For example, although the process of attaching a carbon nanotube strand via arc-discharge or contact method to sharp metal probe is fast, simple and economical it suffers from low yield. Therefore, it is difficult to determine the quality of carbon nanotube strand attached to metal tip unless examined under SEM. When checked under SEM a large percentage of the metal probes have multiple nanotubes attached or clusters of amorphous carbon accompanying the carbon nanotubes [65]. Hence random networks of SWNTs have been explored as an alternative [66].

Nanotube networks take up more space than individual SWNTs, but they are much easier to fabricate and show great promise towards simple mass fabrication of NTFETs. In this second configuration, the devices contain a random array of nanotubes between source and drain electrodes (Fig. 1.4c). In this configuration, current flows along several conducting channels that determine the overall device resistance. The device characteristics depend on the number of nanotubes and density of the nanotube network. It is reported that the conductance drops are associated with junctions formed by crossed semiconducting and metallic nanotubes. Local conductance is more dependent on the number of connections to the specific area; clusters of nanotubes with many paths to the electrode have significantly higher conductance than those parts of the network connected through fewer paths. Areas with low conductance typically only have two to three connections to the network, thus it is likely that these connections are dominated by the presence of highly resistive metallic/semiconducting junctions. When a sufficient back gate voltage is applied to the sample, current flow through the semiconducting tubes is suppressed. Using this technique, differences between metallic and semiconducting SWNT can be distinguished. This type of device configuration, containing a network of conducting nanotube channels, is less sensitive than devices made of single nanotubes. In both types of device configurations, the parameter used for detection is the transfer characteristic – the dependence of either the source-drain current ( $I_{SD}$ ) or conductance ( $G_{SD}$ ) (for a fixed source-drain voltage  $V_{SD}$ ) on the gate voltage ( $V_G$ ) (Fig. 1.4d).

NTFETs can operate as p-type or n-type transistors. The mode of operation can be changed from the pristine p-type to n-type by either adding electron donor molecules (n-doping) or removing adsorbed oxygen by annealing the contacts under vacuum [67]. Polymer-gated NTFETs can also tune their modes of operation: a change in the chemical group of the polymer changes the NTFET from p-type to n-type [68, 69]. Oxygen doping was attributed to the fact that the oxygen interacts with the nanotube–metal junction and causes the p-type characteristic for NTFETs in air by pinning the metal's Fermi level near the nanotube's valance band maximum [33]. However, there is no apparent consensus in the literature about the exact mechanism of chemical sensitivity of NTFETs.



## 1.4

### Sensor Applications of NTFETs

Before discussing NTFET applications for biological detection we first describe the effect of small molecules, relative humidity, and conductive liquid media on NTFET devices characteristics. Effect of these factors should be well understood before NTFET biodetection is reviewed.

#### 1.4.1

#### Sensitivity of NTFETs to Chemical Environment

Generally, the molecular species in the ambient environment have a significant impact on the electrical properties of NTFETs. The conductance of semiconducting SWNTs can be substantially increased or decreased by exposure to  $\text{NO}_2$  or  $\text{NH}_3$  [24]. Exposure to  $\text{NH}_3$  effectively shifts the valance band of the nanotube away from the Fermi level, resulting in hole depletion and reduced conductance. In contrast, on exposure to  $\text{NO}_2$  molecules the conductance of nanotubes increases by three orders of magnitude [70]. Here, exposure of the initially depleted sample to  $\text{NO}_2$  resulted in the nanotube Fermi level shifting closer to the valence band. This caused enriched hole carriers in the nanotube and enhanced sample conductance. These results show that molecular gating effects can shift the Fermi level of semiconducting SWNTs and modulate the resistance of the sample by several orders of magnitude.

The electronic properties of SWNTs are also extremely sensitive to air or oxygen exposure [33]. Isolated semiconducting nanotubes can be converted into apparent metals through room temperature exposure to oxygen. As the surrounding medium was cycled between vacuum and air, a rapid and reversible change in the SWNT resistance occurred in step with the changing environment. Initially, in a pure atmospheric pressure oxygen environment, the thermoelectric power (TEP)  $S$  was positive with a magnitude of nearly  $+20 \text{ mV K}^{-1}$ . This relatively large positive TEP is consistent with that reported for pristine SWNTs near room temperature [71]. As oxygen was gradually removed from the chamber, the TEP changed continuously from positive to negative, with a final equilibrium value of approximately  $-10 \text{ } \mu\text{V K}^{-1}$ . When oxygen was reintroduced into the chamber, the TEP reversed sign and once again became positive. These dramatic 10–15% variations in  $R$  and change in sign of the TEP demonstrate that SWNTs are exceptionally sensitive to oxygen.

In the carbon nanotubes sensors mentioned above, chemical sensing experiments have been conducted with devices in which both nanotubes and nanotube–metal contacts were directly exposed to the environment. The sensing could be dominated by the interaction of molecules with the metal contacts or the contact interfaces. Adsorbed molecules would modify the metal work functions and, thereby, the Schottky barrier [72, 73]. Heinze et al. [64] have assigned the effect of oxygen to the Schottky barrier. Recently, a new device architecture has been studied in which the interface between the metallic contacts and nanotubes is covered by a

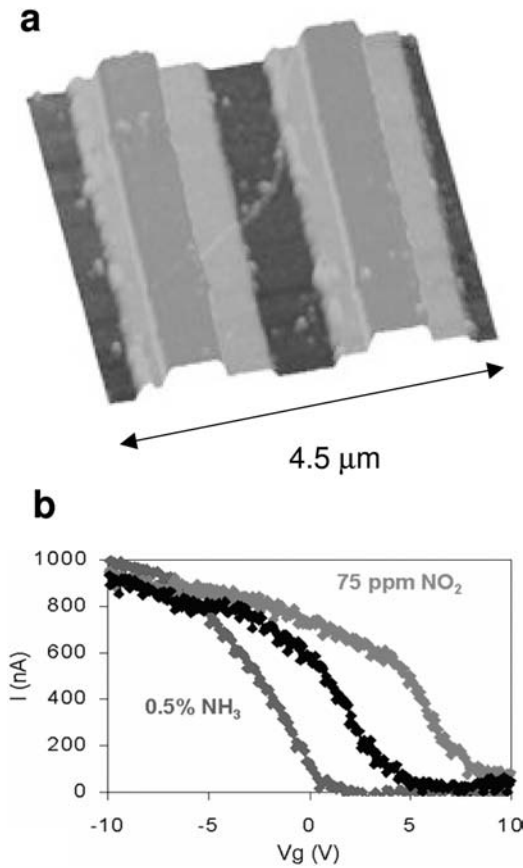


**Fig. 1.5.** (a) AFM image of a contact passivated NTFET device covered with poly(ethylene imine). (b)  $I_{SD}-V_G$  dependence for the device in vacuum (center curve), as well as in  $\text{NH}_3$  and  $\text{NO}_2$  gases. (Adapted with permission from Ref. [74], © 2003 American Institute of Physics).

passivation layer, referred to as contact-passivated [74]. In this configuration, with the junction isolated and only the central length of the nanotube channels exposed, the contacts should be isolated from the effect of chemicals. At the same time, the section of the device that is open to the environment can be doped via charge transfer. NTFETs with such configuration have been investigated by measuring sensitivity to  $\text{NH}_3$ ,  $\text{NO}_2$ , and poly(ethylene imine) (Fig. 1.5).

The NTFET devices were fabricated using SWNTs grown by CVD on 200 nm of silicon dioxide on doped silicon from iron nanoparticles as described in Section 1.3.1. These particles were exposed to flowing hydrocarbon to grow carbon nanotubes, and after growth optical lithography was used to pattern electrical leads (35 nm titanium capped with 5 nm gold) on top of the nanotubes. Contact passiva-

tion was achieved by 70 nm silicon monoxide layer. Source and drain electrodes were separated by nearly a micrometer. The dependence of the source-drain current ( $I_{SD}$ ) as function of the gate voltage ( $V_G$ ) was measured from +10 to -10 V using a semiconductor parameter analyzer in air/water/gas mixtures. The low concentrations of gas mixtures could be introduced to the devices by mixing different proportions of air and gases. The contact-passivated devices demonstrated  $\text{NH}_3$  and  $\text{NO}_2$  sensitivity similar to regular NTFETs. Poly(ethylene imine) also produced negative threshold shifts of tens of volts, despite being in contact with only the center region of devices. Thus, the NTFET sensor character was preserved despite isolating Schottky barriers.

Several groups have reported that NTFET fabricated on  $\text{SiO}_2/\text{Si}$  substrates exhibits hysteresis in current versus gate-voltage characteristics and attributed the hysteresis to charge traps in bulk  $\text{SiO}_2$ , oxygen-related defect trap sites near nanotubes, or the traps at the  $\text{SiO}_2/\text{Si}$  interface. It is mentioned that thermally grown  $\text{SiO}_2$  surface consists of Si-OH silanol groups and is hydrated by a network of water molecules that are hydrogen bonded to the silanols. The CVD nanotube growth condition (900 °C) may dehydrate the surface and condense to form Si-O-Si siloxanes. When such a surface is exposed to and stored in ambient air, the surface siloxanes on the substrate react with water and gradually revert to Si-OH, after which the substrate becomes rehydrated. Heating under dry conditions significantly removes water and reduces hysteresis in the transistors.

Kim et al. have reported that the hysteresis in electrical characteristics of NTFETs is due to charge trapping by water molecules around the nanotubes, including  $\text{SiO}_2$  surface-bound water proximal to the nanotubes [75]. They have demonstrated that coating nanotube devices with PMMA can afford nearly hysteresis-free NTFETs [75]. This passivation is attributed to two factors. First, the ester groups of poly(methyl methacrylate) (PMMA) can hydrogen bond with silanol group on  $\text{SiO}_2$ . Baking at 150 °C combined with the polymer-SiO<sub>2</sub> interaction can significantly remove the silanol-bound water. Second, PMMA is hydrophobic and can keep water in the environment from permeating the PMMA and adsorbing on the nanotube in a significant manner.

Bradley et al. have attributed hysteresis in NTFET devices to cation diffusion [76], based on the following experiments. First, NTFET devices that exhibit very small hysteresis were fabricated. Subsequently, these devices were modified by the addition of an electrolyte coating that created mobile ions on the surface of the device and resulted in the large hysteresis. Experiments were also conducted to explore possible mechanisms for cation-induced hysteresis by varying the humidity that changes the hydration layer around the nanotubes, thus leading to the increase of the ionic mobility. The hysteresis has been found to be sensitive to humidity on sub-second time scales, showing promise as a humidity sensor [77].

Sensitivity of NTFETs to charges as well as NTFET operation in conducting liquid media is important for biosensor design where the sensor should operate in physiological buffers with complex mixtures of biomolecules. Figure 1.6 shows a typical transfer characteristic of NTFET measured in air and water using the silicon and water as the gate electrode, respectively. The change in device characteris-

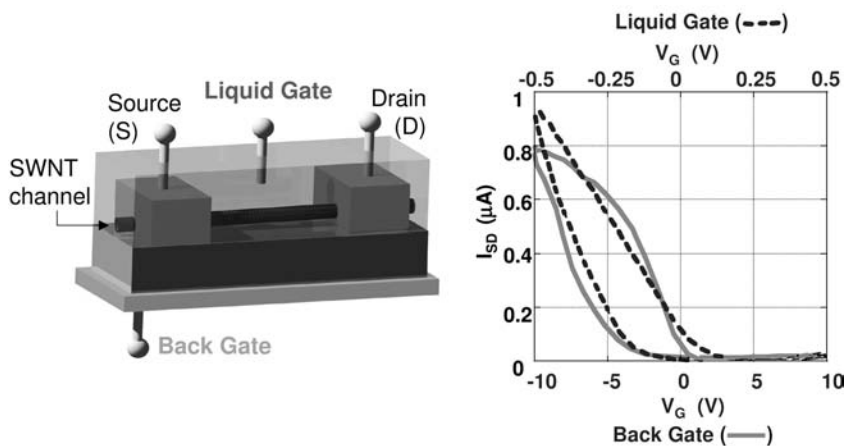


**Fig. 1.6.** (a) Detection in liquid with NTFET devices by using either the back gate or liquid gate configuration. (b) NTFET transfer characteristics in air (solid line), using the back gate, and in water (dashed line), using

the liquid gate. Note the different x-scales for the back and liquid gates. (Adapted with permission from Ref. [93], © 2003, The American Physical Society.)

tics upon exposure to a water/gas mixture is reflected in the transfer characteristics. Saline or electrolytes can also gate NTFETs and give high transconductance [62, 78].

#### 1.4.2

#### Bioconjugates of Carbon Nanotubes

Numerous reports demonstrate the ability to chemically functionalize nanotubes for biological applications [79, 80]. Such chemistry is readily transferable to many applications, ranging from sensors [81, 82] to electronic devices [83]. SWNTs are chemically stable and highly hydrophobic. Therefore, they require surface modification to establish effective SWNT–biomolecule interaction.

So far, two methods of exohedral functionalization of SWNTs have been developed – namely covalent and noncovalent. While covalent modifications [84] are often effective at introducing functionality, they impair the desirable mechanical and electronic properties of SWNTs. Noncovalent modifications [85], however, not only improve the solubility of SWNTs in water, but they also constitute non-destructive processes, which preserve the primary structures of the SWNTs, along with their unique mechanical and electronic properties.

Previously, it has been shown that polysaccharides such as starch [86, 82, 83], gum Arabic [84], and the  $\beta$ -1,3-glucans, curdlan and schizophyllan [85], will solubilize SWNTs in water. It has been proposed that at least some of these polymers achieve their goal by wrapping themselves in helical fashion around SWNTs (Fig.

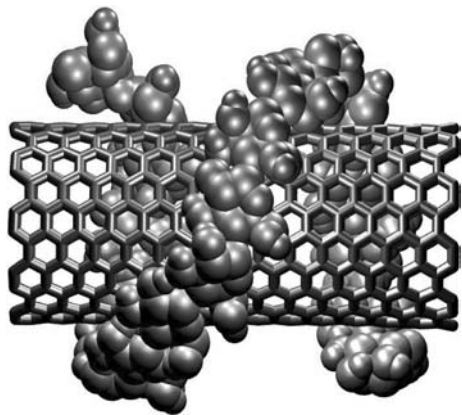


Fig. 1.7. Molecular model of SWNT wrapped in an amylose coil. (Reprinted from Ref. [79], © 2002, The American Chemical Society.)

1.7). Solubilization of the SWNTs with cyclodextrins (CD), which are macrocyclic polysaccharides, has been also investigated [86]. The observed aqueous solubility of SWNTs with  $\gamma$ -CD is unlikely due to encapsulation because the inner cavity dimensions of this CD are far too small to allow it to thread onto even the smallest diameter SWNTs. More recently, however, it has been shown [87] that  $\eta$ -CD, which has 12  $\alpha$ 1,4-linked D-glucopyranose residues and therefore is large enough, does thread onto SWNTs in water, not only solubilizing the NTs but also permitting some partial separations according to their diameters.

Nucleic acids, such as single-stranded DNA, short double-stranded DNA, and some total RNA can also disperse SWNTs in water [88, 89]. Molecular modeling has shown [20] that the non-specific DNA–SWNT interactions in water are from the nucleic acid–base stacking on the nanotube surface, resulting in the hydrophilic sugar–phosphate backbone pointing to the exterior to achieve the solubility in water. The mode of interaction could be helical wrapping or simple surface adsorption. The charge differences among the DNA–SWNT conjugates, which are associated with the negatively charged phosphate groups of DNA and the different electronic properties of SWNTs, have allowed post-production preparation of samples enriched in metallic and semiconducting SWNTs.

Various proteins can also strongly bind to the nanotube exterior surface via non-specific adsorption. Proteins such as streptavidin and HupR crystallize in helical fashion, resulting in ordered arrays of proteins on the nanotube surface [90]. Mechanistically, the non-specific adsorption of proteins onto the nanotube surface may be more complicated than the widely attributed hydrophobic interactions. Quite possibly, the observed substantial protein adsorption is, at least in part, associated with the amino affinity of carbon nanotubes, as was demonstrated recently by monitoring the conductance change in the carbon nanotube [91]. Also, inter-

molecular interactions involving aromatic amino acids, i.e., histidine and tryptophan, in the polypeptide chains of the proteins can contribute to the observed affinity of the peptides to carbon nanotubes [92].

### 1.4.3

#### Protein Detection

Carbon nanotube interactions with proteins have been explored by NTFET devices [91]. In NTFET devices, the ability to measure the electronic properties of the nanotube allowed to query the electronic state of the immobilization substrate. In that work two types of measurements of the device transfer characteristics were performed. In the first measurement, referred to as a substrate-gate transfer characteristic, the current through the drain contact (at fixed source-drain bias) was monitored while a variable gate voltage was applied through a metallic gate buried underneath the SiO<sub>2</sub> substrate. In the second measurement, referred to as liquid-gate transfer characteristics, the device was immersed in a buffer solution and a variable gate voltage was applied through a platinum electrode. The current was passed through the drain contact and a silver reference electrode in the solution. During these measurements, the assembly was shaken gently, using a lab rotator at 3 Hz. The effect of protein adsorption was studied with both measurements. Devices were incubated with streptavidin (40 nm) in 15 mM phosphate buffer at 25 °C. Liquid-gate transfer characteristics were measured continually during the incubations. After 10 h, the devices were rinsed with distilled water and blown dry, and the substrate-gated transfer characteristics of the dried devices were measured.

These results were discussed in terms of a simple model in which adsorbed streptavidin coats the single-walled nanotube (Fig. 1.8). The gradual shift in the threshold voltage is assumed to result from the slow accumulation of a full monolayer of adsorbed protein. This coverage-dependent threshold shift is analogous

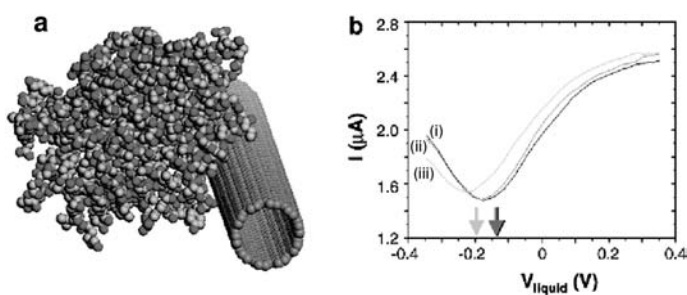


**Fig. 1.8.** (a) Size comparison between a carbon nanotube and a streptavidin molecule. (b) Current versus gate voltage for a nanotube device;  $V_{\text{SD}} = 10$  mV. (ii) In phosphate buffer before streptavidin addition. (i) same conditions, to measure the uncertainty in the

threshold voltage. (iii) After 10 h of incubation with streptavidin. Arrows indicate the threshold voltages for the three curves [the arrow for (i) is behind that for (ii)]. (Adapted with permission from Ref. [91], © 2003, The American Chemical Society.)

to the concentration-dependent shift observed when such devices are exposed to aqueous ammonia [93]. The protein adsorbate equilibrates over several hours so that only the full monolayer can be conclusively determined. Such protein monolayers form under various conditions at interfaces that permit protein crystallization, including sidewalls of MWNTs [90, 94]. The results support the proposal that conductance changes are due to charge injection or field effects caused by proteins adsorbed solely along the lengths of the nanotubes.

Protein adsorption on NTFET leads to appreciable changes in the electrical conductance of the devices that can be exploited for label-free detection of biomolecules with a high potential for miniaturization. For example, Dai and coworkers [95] have used a sensor design consisting of an array of four NTFET sensors on SiO<sub>2</sub>/Si chips. Each NTFET consists of multiple SWNTs connected roughly in parallel across two closely spaced bridging metal electrodes. Three types of devices with different surface functional groups were prepared for the investigation of the biosensing: (1) unmodified as-made devices, (2) devices fabricated with mPEG-SH SAMs formed on, and only on, the metal contact electrodes and, lastly, (3) devices with mPEG-SH SAMs on the metal contacts and a Tween 20 coating on the carbon nanotubes. Electrical conductance of these devices upon the addition of various protein molecules was monitored. While device type 1 showed a significant conductance change with protein adsorption, device type 2 with an mPEG-SH SAM on the metal electrodes did not give any conductance change, except in the case of the protein avidin. It was reported that the metal–nanotube interface or contact region is highly susceptible to modulation by adsorbed species [64]. Modulation of metal work function can alter the Schottky barrier of the metal–nanotube interface, thus leading to a significant change in the nature of contacts and, consequently, a change in the conductance of the devices.

*In situ* detection of a small number of proteins by directly measuring the electron transport properties of a single SWNT has been reported by Nagahara and coworkers [96]. Cytochrome *c* (cytc) adsorption onto individual NTFET has been detected via the changes in the electron transport properties of the transistors. The adsorption of cytc induces a decrease in the conductance of the NTFET devices, corresponding to a few tens of molecules. This experiment was carried out by measuring the conductance versus electrochemical potential of the SWNT with respect to a reference electrode inserted in the solution, and observed a negative shift in the conductance versus potential plot upon protein adsorption. The number of adsorbed proteins has been estimated from this shift.

#### 1.4.4

#### Detection of Antibody–Antigen Interactions

Specific sensitivity can be achieved by employing recognition layers that induce chemical reactions and modify the transfer characteristics. In this two-layer architecture carbon nanotubes function as extremely sensitive transducers while the recognition layer provides chemical selectivity and prevents non-specific binding that is common for complex biological samples.

Following this design, nanotubes have been functionalized to be biocompatible and to be capable of recognizing proteins. This functionalization has involved noncovalent binding between a bifunctional molecule and a nanotube to anchor a bioreceptor molecule with a high degree of control and specificity. Star and co-workers have fabricated [97] NTFET devices sensitive to streptavidin using a biotin-functionalized carbon nanotube bridging two microelectrodes (source and drain, Fig. 1.9a). The SWNT in the NTFET device was coated with a mixture of two polymers, poly(ethyleneimine) and poly(ethylene glycol). The former provided amino groups for the coupling of biotin-*N*-hydroxysuccinimide ester (Fig. 1.9b) and the latter prevented the nonspecific adsorption of proteins on the functionalized carbon nanotube. Figure 1.9(c) shows an AFM image of the device after its exposure to streptavidin labeled with gold nanoparticles (10 nm). Lighter dots represent gold nanoparticles and indicate the presence of streptavidin bound to the

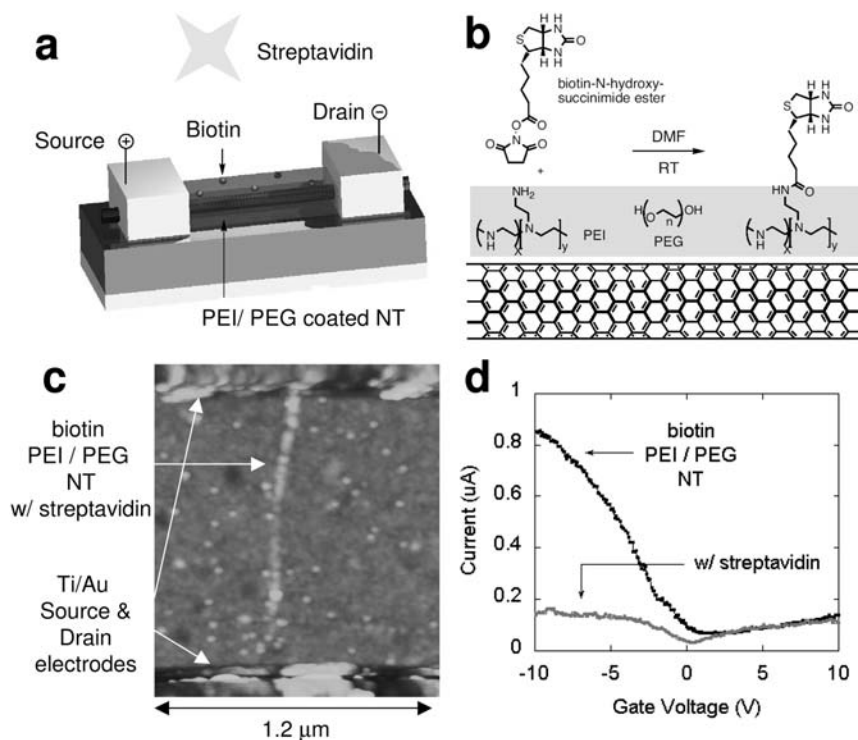


**Fig. 1.9.** (a) Schematic of NTFET coated with a biotinylated polymer layer for specific streptavidin binding. (b) Biotinylation reaction of the polymer layer (PEI/PEG) on the side-wall of the SWNT. (c) AFM image of the polymer-coated and biotinylated NTFET device after exposure to streptavidin labeled with gold

nanoparticles (10 nm in diameter). (d) Source-drain current dependence on gate voltage of the NTFET device based on SWNTs functionalized with biotin in both the absence and presence of streptavidin. (Adapted with permission from Ref. [97], © 2003, The American Chemical Society.)



biotinylated carbon nanotube. The source-drain current dependence on the gate voltage of the NTFET shows a significant change upon the streptavidin binding to the biotin-functionalized carbon nanotube (Fig. 1.9d). The experiments reveal the specific binding of the streptavidin, which occurs only at the biotinylated interface.

The mechanism of the biodetection was explained in terms of the effect of the electron doping of the carbon nanotube channel upon the binding of the charged streptavidin molecules. Dai and coworkers [98] have also analyzed specific antigen–antibody interactions using NTFET devices. In particular, they have studied the affinity binding of 10E3 mAbs antibody (a prototype target of the autoimmune response in patients with systematic lupus erythematosus and mixed connective tissue disease) to human auto antigen U1A.

#### 1.4.5

##### **DNA Detection**

DNA biosensors based on nucleic acid recognition processes are quickly being developed towards the goal of rapid, simple and inexpensive testing of genetic and infectious diseases. To date, there are several reports on the electrochemical detection of DNA hybridization using multi-walled carbon nanotube (MWNT) electrodes [99]. Whereas electrochemical methods rely on the electrochemical behavior of the labels, measurements of the direct electron transfer between SWNTs and DNA molecules paves the way for label-free DNA detection (Fig. 1.10). To illustrate the practical utility of this new nanoelectronic detection method, an allele-specific assay to detect the presence of SNPs using NTFETs has been recently developed [100]. This DNA assay targeted the H63D polymorphism in the human HFE gene, which is associated with hereditary hemochromatosis, a common and easily treated disease of iron metabolism [101, 102].

DNA sensing mechanism using NTFETs has been recently explored by selective attachment of DNA molecules at different device segments. Tang et al. [103] have found that DNA hybridization on gold electrodes rather than on SWNT sidewalls is mainly responsible for NTFET detection due to Schottky barrier modulation. In another approach, DNA hybridization occurs on the surface at the gate of NTFET [104]. As a result, the conductance in SWNTs was changed through the gate insulators. In the work, the 5' end-amino modified peptide nucleic acid (PNA) oligonucleotides were covalently immobilized onto the Au surfaces of the back gate of NTFETs. PNA is a synthetic analog of DNA, in which both the phosphate and the deoxyribose of the DNA backbone are replaced by a polypeptide. PNA mimics the behavior of DNA and hybridizes with complementary DNA or RNA sequences, thus enabling PNA chips to be used in biosensors. The micro-flow chip was fabricated by using poly(dimethylsiloxane) (PDMS) prepolymer. The NTFET nano-sensor array was placed onto the PDMS chip in such a way that the PNA probe-modified Au side was positioned to face the open chamber for the introduction of solutions and the electrical measurements. A PNA probe with the base sequence 5'-NH<sub>2</sub>-ACC ACC ACT TC-3', which was fully complementary to the tumor necro-

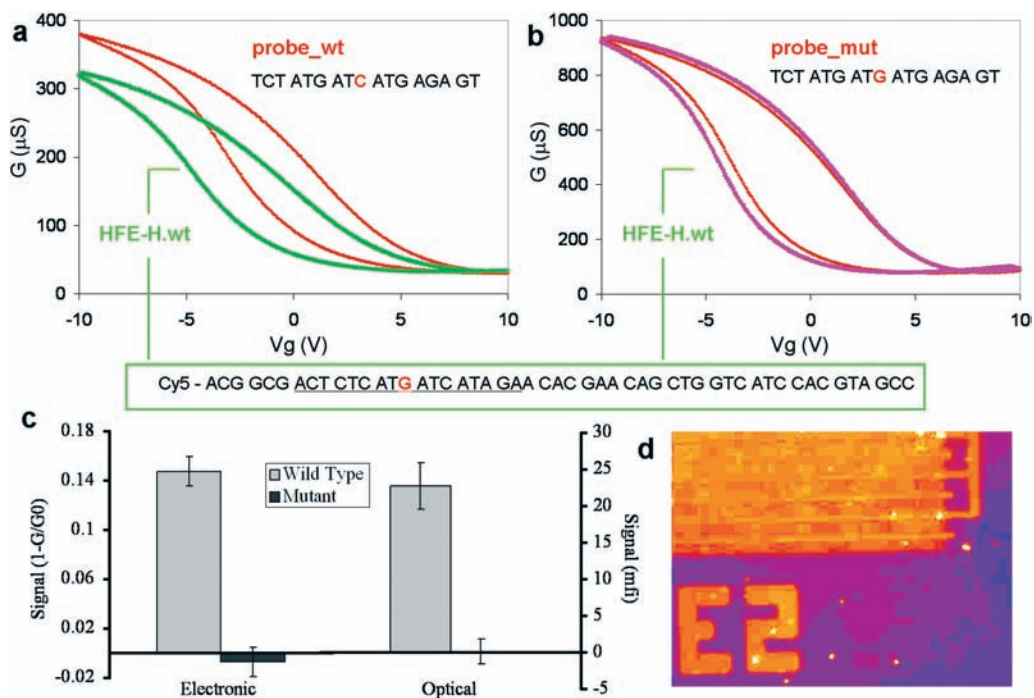


**Fig. 1.10.** Label-free detection of DNA hybridization using NTFET devices. (a)  $G-V_g$  curves after incubation with allele-specific wild-type capture probe and after challenging the device with wild-type synthetic HFE target (50 nm). (b)  $G-V_g$  curves in the experiment with mutant capture probe. (c) Graph with electronic ( $1 - G/G_0$ ) and fluorescent

responses in SNP detection assays. (d) Fluorescence microscopy image of the NTFET network device, with the electrodes 10 mm apart, after incubation with Cy5-labeled DNA molecules. (Adapted with permission from Ref. [100], © 2006, The National Academy of Sciences of the USA.)

sis factor- $\alpha$  (TNF- $\alpha$ ) gene sequence, was used as a model system. The base sequence for full complementary target DNA was 5'-GGT TTC GAA GTG GTG GTC TTG-3' while the non-complementary DNA oligonucleotide sequence was 5'-CCC TAA GCC CCC AA-3'.

The electrical properties of the NTFET devices were measured at room temperature in air. First, the blank PBS solution was introduced into the PDMS-based micro flow chip, revealing that no substantial change in the source-drain current of NTFET was obtained. The current increased dramatically while monitoring in real time for about 3 h. The increase in conductance for the p-type NTFET device was consistent with an increase in negative surface charge density associated with binding of negatively charged oligonucleotides at the surface. DNA hybridization can be detected by measuring the electrical characteristics of NTFETs, and SWNT based FET can be employed for label-free, direct real time electrical detection of biomolecule binding.

## 1.4.6

**Enzymatic Reactions**

SWNTs can be made water soluble by wrapping in amylose (linear component of starch) [86]. These SWNT solutions are stable for weeks, provided nobody spits on them. Indeed, the addition of saliva, which contains  $\alpha$ -amylase, precipitates the nanotubes as the enzyme breaks amylose down into smaller carbohydrate fragments, finally resulting in the formation of glucose. The enzymatic degradation of starch has been recently monitored electronically using NTFETs [105]. Figure 1.11(a) shows the experimental setup used for this study. NTFET devices display transconductance and source-drain current–voltage characteristics typical of the p-type device behavior. The device characteristics, i.e., the source-drain current  $I_{SD}$  as a function of the gate voltage  $V_G$ , were measured to evaluate the effect of starch deposition and the subsequent enzymatic degradation of the starch layer on the carbon nanotubes.

Starch was deposited onto the FET by soaking the silicon wafer in a 5% aqueous starch solution and the device characteristics were found to be shifted by approxi-

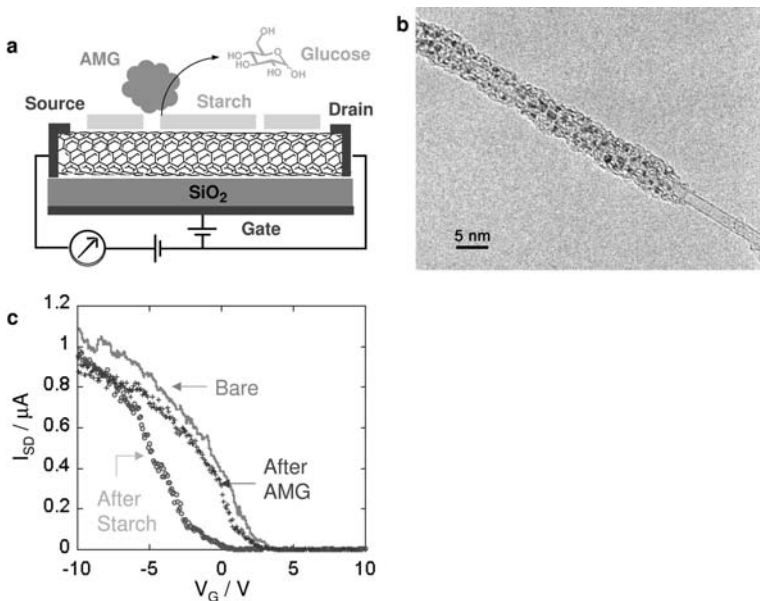


**Fig. 1.11.** (a) NTFET device for electronic monitoring of the enzymatic degradation of starch with amyloglucosidase (AMG) to glucose. (b) High-resolution transmission electron microscopy (HRTEM) image of a SWNT (2.0 nm diameter) after treatment with a drop of a 1% of an aqueous solution of starch. The starch had been stained with  $\text{RuO}_4$

vapor. (c) NTFET device characteristics in the form of  $I_{SD}-V_G$  curves measured from +10 to  $-10$  V gate voltage with a +0.6 V bias voltage before (bare) and after starch deposition, as well as after hydrolysis with AMG. (Adapted with permission from Ref. [104], © 2004, The American Chemical Society.)

mately 2 V toward more negative gate voltages. The direction of the shift equates with electron doping of the nanotube channel by the polysaccharide. Quantitatively similar doping effects have been observed when carbon nanotube FET devices were exposed to  $\text{NH}_3$  gas, amines [106], poly(ethylene imine) (PEI) [107], and proteins [91]. After the enzyme-catalyzed reaction had been performed on the starch-functionalized devices and washed with buffer, the  $I_{SD}$  vs.  $V_G$  characteristics recovered almost completely to the trace recorded before starch deposition (Fig. 1.11). This indicates that, during the enzyme-catalyzed reaction, nearly all the starch deposited on the surface of the nanotube device is hydrolyzed to glucose which is washed off by the buffer prior to the electronic measurements.

#### 1.4.7

##### Glucose Detection

The diagnosis and management of diabetes mellitus requires a tight monitoring of blood glucose levels. Dekker and coworkers have demonstrated the use of individual semiconducting SWNT as a versatile biosensor [108]. The redox enzyme glucose oxidase ( $\text{GO}_x$ ) that catalyses the oxidation of  $\beta$ -D-glucose ( $\text{C}_6\text{H}_{12}\text{O}_6$ ) to D-glucono-1,5-lactone ( $\text{C}_6\text{H}_{10}\text{O}_6$ ) has been studied. The redox enzymes go through a catalytic reaction cycle where groups in the enzyme temporarily change their charge state and conformational changes occur in the enzyme that can be detected using NTFET devices.

In addition to pH sensitivity,  $\text{GO}_x$ -coated semiconducting SWNTs appeared to be sensitive to glucose, the substrate of  $\text{GO}_x$ . Figure 1.12 exhibits real-time measure-

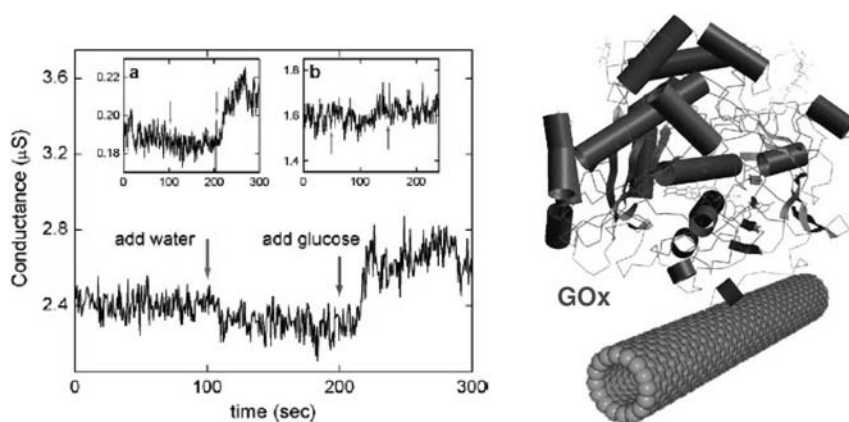


**Fig. 1.12.** Real time electronic response of the NTFET sensor to glucose, the substrate of glucose oxidase ( $\text{GO}_x$ ). The conductance of a semiconducting SWNT with immobilized  $\text{GO}_x$  is measured as a function of time in 5  $\mu\text{L}$  milli-Q water. The conductance of the  $\text{GO}_x$ -coated SWNT increases upon addition of glucose to the liquid. Inset: (a) the same measurement on

a second device where the conductance was a factor of 10 lower; (b) the same measurement on a semiconducting SWNT without  $\text{GO}_x$ ; no conductance increase is observed in this case. (Reprinted with permission from Ref. [107], © 2003, The American Chemical Society.) (B) Schematic of  $\text{GO}_x$  immobilized on SWNT for electronic glucose detection.

ments where the conductance of a GOx-coated semiconducting SWNT in milli-Q water has been recorded in the liquid (left-hand arrow in each graph in Fig. 1.12). No significant change in conductance was observed as a result of water addition. When 0.1 M glucose in milli-Q water was added to the liquid (right-hand arrow in each graph), however, the conductance of the tube increased by about 10%. A similar 10% conductance change was observed for another device (Fig. 1.12a inset), which had a factor 10 lower conductance. Glucose did not change the conductance of the bare SWNT but did increase the device conductance after GOx was immobilized. Inset (b) of Fig. 1.12 shows such measurement on a bare semiconducting SWNT. These measurements clearly indicate that the GOx activity is responsible for the observed increase in conductance upon glucose addition, thus rendering such nanodevices as feasible enzymatic-activity sensors.

## 1.5

### Conclusion and Outlook

Recent advances in the rapidly developing area of biomolecule detection using carbon nanotube systems have been summarized here. SWNTs appear as structurally defined components for various electronic devices. The semiconductive properties of SWNTs are of special interest as these SWNTs have been applied to fabricate FETs for sensing applications. This area requires further development, particularly related to the fabrication of FETs based on individual SWNTs. The use of carbon nanotubes as nanocircuitry elements is particularly interesting. Biomaterials linked to nanotubes may be used as binding elements for the specific linkage of the nanotube to surface in the form of addressable structures.

Important chemical means to functionalize SWNTs with other electronic materials such as conductive polymers or nanoparticles is anticipated to generate materials of new properties and functions. The localized nanoscale contacts of SWNTs with bio-surfaces will be a major advance in understanding and exploring the new applications. The use of nanodevices to monitor various biologically significant reactions is envisioned. In future, it should be possible to connect the living cells directly to these nanoelectronic devices to measure the electronic responses of living systems. The combination of the unique electronic properties of SWNTs and catalytic features of biological system could provide new opportunities for carbon nanotubes based bioelectronics.

### References

- 1 PARK, S., TATON, T. A., MIRKIN, C. A. Array-based electrical detection of DNA with nanoparticle probes., *Science* **2002**, 295, 1503–1506.
- 2 HE, L., MUSICK, M. D., NICEWARNER, S. R., SALINAS, F. G., BENKOVIC, S. J., NATAN, M. J., KEATING, C. D. Colloidal Au-enhanced surface plasmon resonance for ultrasensitive detection of DNA hybridization., *J. Am. Chem. Soc.* **2000**, 122, 9071–9077.

- 3 MCFARLAND, A. D., VAN DUYN, R. P. Single silver nanoparticles as real-time optical sensors with zeptomole sensitivity., *Nano Lett.* **2003**, *3*, 1057–1062.
- 4 GRAHAM, A. P., DUESBERG, G. S., SEIDEL, R. V., LIEBAU, M., UNGER, E., PAMLER, W., KREUPL, F., HOENLEIN, W. Carbon nanotubes for microelectronics?, *Small* **2005**, *1*, 382–390.
- 5 GRÜNER, G. Carbon nanotube transistors for biosensing applications., *Anal. & Bioanal. Chem.*, **2006**, *384*, 322–335.
- 6 WILLNER, I. Biomaterials for sensors, fuel cells, and circuitry., *Science* **2002**, *298*, 2407–2408.
- 7 CUI, Y., WEI, Q., PARK, H., LIEBER, C. M. Nanowire nanosensors for highly sensitive and selective detection of biological and chemical species., *Science* **2001**, *293*, 1289–1292.
- 8 HAHM, J., LIEBER, C. M. Direct ultrasensitive electrical detection of DNA and DNA sequence variations using nanowire nanosensors., *Nano Lett.* **2004**, *4*, 51–54.
- 9 PATOLSKY, F., ZHENG, G., HAYDEN, O., LAKADAMYALI, M., ZHUNG, X., LIEBER, C. M. Electrical detection of single viruses, *Proc. Natl. Acad. Sci. U.S.A.* **2004**, *101*, 14017–14022.
- 10 WEISS, S. Measuring conformational dynamics of biomolecules by single molecule fluorescence spectroscopy., *Nat. Struct. Biol.* **2000**, *7*, 724–729.
- 11 ZHUANG, X. W., RIEF, M. Single-molecule folding., *Curr. Opin. Struct. Biol.* **2003**, *13*, 88–97.
- 12 AJAYAN, P. M. Nanotubes from carbon., *Chem. Rev.* **1999**, *99*, 1787–1799.
- 13 AJAYAN, P. M., ZHOU, O. Z. Applications of carbon nanotubes., *Top. Appl. Phys.* **2001**, *80*, 391–425.
- 14 Special issue on carbon nanotubes, *Acc. Chem. Res.* **2002**, vol. 35.
- 15 WANG, J. Carbon-nanotube based electrochemical biosensors: A review., *Electroanalysis* **2005**, *17*, 7–14.
- 16 LIN, Y., TAYLOR, S., LI, H., SHIRAL FERNANDO, K. A., QU, L., WANG, W., GU, L., ZHOU, B., SUN, Y. P. Advances toward bioapplications of carbon nanotubes., *J. Mater. Chem.* **2004**, *14*, 527–541.
- 17 KATZ, E., WILLNER, I. Biomolecule-functionalized carbon nanotubes: applications in nanobioelectronics., *ChemPhysChem* **2004**, *5*, 1084–1104.
- 18 IJIMA, S. Helical microtubules of graphitic carbon., *Nature (London)* **1991**, *354*, 56–58.
- 19 DRESSSELHAUS, M. S., DRESSSELHAUS, G., EKLUND, P. C. *Science of Fullerenes and Carbon Nanotubes*, Academic Press, San Diego, **1996**.
- 20 SAITO, R., DRESSSELHAUS, G., DRESSSELHAUS, M. S. *Physical Properties of Carbon Nanotubes*, Imperial College Press, London, **1999**.
- 21 DE JONGE, N., LAMY, Y., SCHOOTS, K., OOSTERKAMP, T. H. High brightness electron beam from a multi-walled carbon nanotube, *Nature (London)* **2002**, *420*, 393–395.
- 22 FRANSEN, M. J., VAN ROOY, Th. L., KRUIT, P. Field emission energy distributions from individual multiwalled carbon nanotubes., *Appl. Surf. Sci.* **1999**, *146*, 312–327.
- 23 WANG, Z. L., PONCHARAL, P., DE HEER, W. A. Measuring physical and mechanical properties of individual carbon nanotubes by in situ TEM., *J. Phys. Chem. Solids* **2000**, *61*, 1025–1030.
- 24 KONG, J., FRANKLIN, N. R., ZHOU, C. W., CHAPLINE, M. G., PENG, S., CHO, K., DAI, H. Nanotube molecular wires as chemical sensors., *Science* **2000**, *287*, 622–625.
- 25 SUGIE, H., TANEMURA, M., FILIP, V., IWATA, K., TAKAHASHI, K., OKUYAMA, F. Carbon nanotubes as electron source in an x-ray tube., *Appl. Phys. Lett.* **2001**, *78*, 2578–2580.
- 26 BAUGHMAN, R. H., ZAKHIDOV, A., DE HEER, W. A. Carbon nanotubes – the route toward applications., *Science* **2002**, *297*, 787–792.
- 27 DEKKER, C. Carbon nanotubes as molecular quantum wires., *Phys. Today* **1999**, *52*, 22–28.
- 28 MCEUEN, P. L., FUHRER, M. S., PARK, H. Single-walled carbon nanotube electronics., *IEEE Trans. Nanotechnol.* **2002**, *1*, 78–85.

- 29 DRESSELHAUS, M. S. Burn and interrogate., *Science* **2001**, 292, 650–651.
- 30 TANS, S. J., VERSCHUEREN, A. R. M., DEKKER, C. Room-temperature transistor based on a single carbon nanotube., *Nature* **1998**, 393, 49–52.
- 31 VALENTINI, L., ARMENTANO, I., KENNY, J. M., CANTALINI, C., LOZZI, L., SANTUCCI, S. Sensor for sub-ppm NO<sub>2</sub> gas detection based on carbon nanotube thin films., *Appl. Phys. Lett.* **2003**, 82, 961–963.
- 32 LI, J., LU, Y. J., YE, Q., CINKE, M., HAN, J., MEYYAPPAN, M. Carbon nanotube sensors for gas and organic vapor detection, *Nano Lett.* **2003**, 3, 929–933.
- 33 COLLINS, P. G., BRADLEY, K., ISHIGAMI, M., ZETTL, A. Extreme oxygen sensitivity of electronic properties of carbon nanotubes., *Science* **2000**, 287, 1801–1804.
- 34 SINNOTT, S. B., ANDREWS, R. Carbon nanotubes: Synthesis, properties, and applications., *Crit. Rev. Solid State Mater. Sci.* **2001**, 26, 145–249.
- 35 KOKAI, F., TAKAHASHI, K., YUDASAKA, M., YAMADA, R., ICHIHASHI, T. and IJIMA, S. Laser ablation of graphite-Co/Ni and growth of single-wall carbon nanotubes in vortexes formed in an Ar atmosphere, *J. Phys. Chem. B* **2000**, 104, 6777–6784.
- 36 TAKIZAWA, M., BANDOW, S., YUDASAKA, M., ANDO, Y., SHIMOYAMA, H., IJIMA, S. Change of tube diameter distribution of single-wall carbon nanotubes induced by changing the bimetallic ratio of Ni and Y catalysts., *Chem. Phys. Lett.* **2000**, 326, 351–357.
- 37 LI, Y., KIM, W., ZHANG, Y., ROLANDI, M., WANG, W., DAI, H. Growth of single-walled carbon nanotubes from discrete catalytic nanoparticles of various sizes., *J. Phys. Chem. B* **2001**, 105, 11 424–11 431.
- 38 IJIMA, S., ICHIHASHI, T. Single-shell carbon nanotubes of 1-nm diameter., *Nature (London)* **1993**, 363, 603–605.
- 39 BETHUNE, D. S., KIANG, C. H., DE VIRE, M. S., GORMAN, G., SAVOY, R., VAZQUEZ, J., BEYERS, R. Cobalt-catalysed growth of carbon nanotubes with single-atomic-layer walls, *Nature (London)* **1993**, 363, 605–607.
- 40 SERAPHIN, S., ZHOU, D. Single-walled carbon nanotubes produced at high yield by mixed catalyst, *Appl. Phys. Lett.* **1994**, 64, 2087–2089.
- 41 WILLEMS, I., KÓNYA, Z., COLOMER, J.-F., VAN TENDELOO, G., NAGARAJU, N., FONSECA, A. and NAGY, J. B. Control of the outer diameter of thin carbon nanotubes synthesized by catalytic decomposition of hydrocarbon, *Chem. Phys. Lett.* **2000**, 317, 71–76.
- 42 HATA, K., FUTABA, D. N., MIZUNO, K., NAMAI, T., YUMURA, M., IJIMA, S. Water-assisted highly efficient synthesis of impurity-free single-walled carbon nanotubes., *Science* **2004**, 306, 1362–1364.
- 43 JOSELEVICH, E., LIEBER, C. M. Vectorial growth of metallic and semiconducting single-wall carbon nanotubes, *Nano Lett.* **2002**, 2, 1137–1141.
- 44 URAL, A., LI, Y., DAI, H. Electric-field-aligned growth of single-walled carbon nanotubes on surfaces., *Appl. Phys. Lett.* **2002**, 81, 3464–3466.
- 45 GAO, J., YU, A., ITKIS, M. E., BEKYAROVA, E., ZHAO, B., NIYOGI, S., HADDON, R. C. Large-scale fabrication of aligned single-walled carbon nanotube array and hierarchical single-walled carbon nanotube assembly., *J. Am. Chem. Soc.* **2004**, 126, 16 698–16 699.
- 46 SU, M., LI, Y., MAYNOR, B., BULDUM, A., LU, J. P., LIU, J. Lattice-oriented growth of single-walled carbon nanotubes, *J. Phys. Chem. B* **2000**, 104, 6505–6508.
- 47 ISMAOH, A., SERGEV, L., WACHTEL, E., JOSELEVICH, E. Atomic-step-templated formation of single wall carbon nanotube patterns, *Angew. Chem, Int. Ed.* **2004**, 43, 6140–6143.
- 48 QIAN, D., WAGNER, G. J., LIU, W. K., YU, M. F., RUOFF, R. S. Mechanics of carbon nanotubes., *Appl. Mechanics Rev.* **2002**, 55, 495–533.
- 49 DURKÖP, T., Electronic Properties of carbon nanotubes studied in field-effect transistor geometries, PhD thesis 2004.

- 50 MARTEL, R., SCHMIDT, T., SHEA, H. R., HERTEL, T., AVOURIS, Ph. Single- and multi-wall carbon nanotube field-effect transistors., *Appl. Phys. Lett.* **1998**, *73*, 2447–2449.
- 51 FUHRER, M. S., KIM, B. M., CHEN, Y. F., DURKÖP, T., BRINTLINGER, T. High-mobility nanotube transistor memory., *Nano Lett.* **2002**, *2*, 755–759.
- 52 JAVEY, A., GUO, J., WANG, Q., LUNDSTROM, M., DAI, H. Ballistic carbon nanotube field-effect transistors, *Nature* **2003**, *424*, 654–657.
- 53 DURKÖP, T., GETTY, S. A., COBAS, E., FUHRER, M. S. Extraordinary mobility in semiconducting carbon nanotubes., *Nano Lett.* **2004**, *4*, 35–39.
- 54 THESS, A., LEE, R., NIKOLAEV, P., DAI, H., PETIT, P., ROBERT, J., XU, C., LEE, Y. H., KIM, S. G., RINZLER, A. G., COLBERT, D. T., SCUSERIA, G. E., TOMANEK, D., FISHER, J. E., SMALLEY, R. E. Crystalline ropes of metallic carbon nanotubes, *Science* **1996**, *273*, 483–487.
- 55 BRONIKOWSKI, M. J., WILLIS, P. A., COLBERT, D. T., SMITH, K. A., SMALLEY, R. E. Gas-phase production of carbon single-walled nanotubes from carbon monoxide via the HiPco process: A parametric study., *J. Vac. Sci. Technol. A* **2001**, *19*, 1800–1805.
- 56 DIEHL, M. R., YALIRAKI, S. N., BECKMAN, R. A., BARAHONA, M., HEATH, J. R. Self-assembled, deterministic carbon nanotube wiring networks., *Angew. Chem. Int. Ed.* **2002**, *41*, 353–356.
- 57 MARTEL, R., DERYCKE, V., LAVOIE, C., APPENZELLER, J., CHAN, K. K., TERSOFF, J., AVOURIS, Ph. Ambipolar electrical transport in semiconducting single-wall carbon nanotubes., *Phys. Rev. Lett.* **2001**, *87*, 256805-1–256805-4.
- 58 BOCKRATH, M., COBDEN, D. H., LIU, J., RINZLER, A. G., SMALLEY, R. E., BALENTS, L., MCEUEN, P. L. Luttinger-liquid behaviour in carbon nanotubes., *Nature* **1999**, *397*, 598–601.
- 59 HU, L., HECHT, D. S., GRÜNER, G. Percolation in transparent and conducting carbon nanotube networks., *Nano Lett.* **2004**, *4*, 2513–2517.
- 60 RADOSAVLJEVIC, M., FREITAG, M., THADANI, K. V., JOHNSON, A. T. Nonvolatile molecular memory elements based on ambipolar nanotube field effect transistors., *Nano Lett.* **2002**, *2*, 761–764.
- 61 APPENZELLER, J., KNOCH, J., DERYCKE, V., MARTEL, R., WIND, S., AVOURIS, Ph. Field-modulated carrier transport in carbon nanotube transistors., *Phys. Rev. Lett.* **2002**, *89*, 126801-1–126801-4.
- 62 ROSENBLATT, S., YAISH, Y., PARK, J., GORE, J., SAZONOVA, V., MCEUEN, P. L. High performance electrolyte gated carbon nanotube transistors., *Nano Lett.* **2002**, *2*, 869–872.
- 63 ZHANG, Y., DAI, H. Formation of metal nanowires on suspended single-walled carbon nanotubes, *Appl. Phys. Lett.* **2000**, *77*, 3015–3017.
- 64 HEINZE, S., TERSOFF, J., MARTEL, R., DERYCKE, V., APPENZELLER, J., AVOURIS, Ph. Carbon nanotubes as Schottky barrier transistors., *Phys. Rev. Lett.* **2002**, *89*, 106801-1–106801-4.
- 65 DE JONGE, N., VAN DRUTEN, N. J. Field emission from individual multiwalled carbon nanotubes prepared in an electron microscope., *Ultramicroscopy* **2003**, *95*, 85–91.
- 66 STADERMANN, M., PAPADAKIS, S. J., FALVO, M. R., NOVAK, J., SNOW, E., FU, Q., LIU, J., FRIDMAN, Y., BOLAND, J. J., SUPERFINE, R., WASHBURN, S. Nanoscale study of conduction through carbon nanotube networks., *Phys. Rev. B* **2004**, *69*, 201402-1–201402-3.
- 67 DERYCKE, V., MARTEL, R., APPENZELLER, J., AVOURIS, Ph. Controlling doping and carrier injection in carbon nanotube transistors., *Appl. Phys. Lett.* **2002**, *80*, 2773–2775.
- 68 LU, C., FU, Q., HUANG, S., LIU, J. Polymer electrolyte-gated carbon nanotube field-effect transistor., *Nano Lett.* **2004**, *4*, 623–627.
- 69 SIDDISONS, G. P., MERCHIN, D., BACK, J. H., JEONG, J. K., SHIM, M. Highly efficient gating and doping of carbon nanotubes with polymer electrolytes., *Nano Lett.* **2004**, *4*, 927–931.
- 70 MARTEL, R., SCHMIDT, T., SHEA, H. R., HERTEL, T., AVOURIS, Ph. Single- and



- multi-wall carbon nanotube field-effect transistors., *Appl. Phys. Lett.* **1998**, *73*, 2447–2449.
- 71 HONE, J., ELLWOOD, I., MUNO, M., MIZEL, A., COHEN, M. L., ZETTL, A., RINZLER, A. G., SMALLEY, R. E. Thermoelectric power of single-walled carbon nanotubes., *Phys. Rev. Lett.* **1998**, *80*, 1042–1045.
- 72 NAKANISHI, T., BACHTOLD, A., DEKKER, C. Transport through the interface between a semiconducting carbon nanotube and a metal electrode., *Phys. Rev. B* **2002**, *66*, 073 307-1–073 307-4.
- 73 FREITAG, M., JOHNSON, A. T., KALININ, S., BONNELL, D. Role of single defects in electronic transport through carbon nanotube field-effect transistors., *Phys. Rev. Lett.* **2002**, *89*, 216 801-1–216 801-4.
- 74 BRADLEY, K., GABRIEL, J.-C. P., STAR, A., GRÜNER, G. Short-channel effects in contact-passivated nanotube chemical sensors., *Appl. Phys. Lett.* **2003**, *83*, 3821–3823.
- 75 KIM, W., JAVERY, A., VERMESH, O., WANG, Q., LI, Y., DAI, H. Hysteresis caused by water molecules in carbon nanotube field-effect transistors., *Nano Lett.* **2003**, *3*, 193–198.
- 76 BRADLEY, K., CUMINGS, J., STAR, A., GABRIEL, J.-C. P., GRÜNER, G. Influence of mobile ions on nanotube based FET devices., *Nano Lett.* **2003**, *3*, 639–641.
- 77 STAR, A., HAN, T.-R., JOSHI, V., STETTER, J. R. Sensing with nafion coated carbon nanotube field-effect transistors., *Electroanalysis* **2004**, *16*, 108–112.
- 78 KRUGER, M., BUITELAAR, M. R., NUSSBAUMER, T., SCHONENBERGER, C., FORRO, L. Electrochemical carbon nanotube field-effect transistor., *Appl. Phys. Lett.* **2001**, *78*, 1291–1293.
- 79 DAGANI, R. DNA matches., *Chem. Eng. News* **2002**, *80*, 8.
- 80 KIM, O.-K., JE, J., BALDWIN, J. W., KOOI, S., PEHRSSON, P. E., BUCKLEY, L. Solubilization of single-wall carbon nanotubes by supramolecular encapsulation of helical amylose., *J. Am. Chem. Soc.* **2003**, *125*, 4426–4427.
- 81 BANDYOPADHYAYA, R., NATIV-ROTH, E., REGEV, O., YERUSHALMI-ROZEN, R. Stabilization of individual carbon nanotubes in aqueous solutions., *Nano Lett.* **2002**, *2*, 25–28.
- 82 NUMATA, M., ASAI, M., KANEKO, K., HASEGAWA, T., FUJITA, N., KITADA, Y., SAKURAI, K., SHINKAI, S. Curdlan and schizophyllan (beta-1,3-glucans) can entrap single-wall carbon nanotubes in their helical superstructure, *Chem. Lett.* **2004**, *33*, 232–233.
- 83 CHEN, J., DYER, M. J., YU, M.-F. Cyclodextrin-mediated soft cutting of single-walled carbon nanotubes., *J. Am. Chem. Soc.* **2001**, *123*, 6201–6202.
- 84 CHEN, J., HAMON, M. A., HIU, H., CHEN, Y., RAO, A. M., EKLUND, P. C., HADDON, R. C. Solution properties of single-walled carbon nanotubes., *Science* **1998**, *282*, 95–98.
- 85 STAR, A., STODDART, J. F., STEUERMAN, D., DIEHL, M., BOUKAI, A., WONG, E. W., YANG, X., CHUNG, S. W., HEATH, J. R. Preparation and properties of polymer-wrapped single-walled carbon nanotubes., *Angew. Chem. Int. Ed.* **2001**, *40*, 1721–1725.
- 86 STAR, A., STEUERMAN, D. W., HEATH, J. R., STODDART, J. F. Starched carbon nanotubes., *Angew. Chem. Int. Ed.* **2002**, *41*, 2508–2512.
- 87 DODZIUK, H., EJCHART, A., ANCZEWSKI, W., UEDA, H., KRINICHNAYA, E., DOLGONOS, G., KUTNER, W. Water solubilization, determination of the number of different types of single-wall carbon nanotubes and their partial separation with respect to diameters by complexation with  $\eta$ -cyclodextrin., *Chem. Commun.* **2003**, 986–987.
- 88 ZHENG, M., JAGOTA, A., SEMKE, E. D., DINER, B. A., MCLEAN, R. S., LUSTIG, S. R., RICHARDSON, R. E., TASSI, N. G. DNA-assisted dispersion and separation of carbon nanotubes., *Nat. Mater.* **2003**, *2*, 338–342.
- 89 ZHENG, M., JAGOTA, A., STRANO, M. S., SANTOS, A. P., BARONE, P., CHOU, S. G., DINER, B. A., DRESSELHAUS, M. S., MCLEAN, R. S., ONOA, G. B., SAMSONIDZE, G. G., SEMKE, E. D., USREY, M., WALLS, D. J. Structure-

- based carbon nanotube sorting by sequence-dependent DNA assembly., *Science* **2003**, 302, 1545–1548.
- 90 BALAVOINE, F., SCHULTZ, P., RICHARD, C., MALLOUH, V., EBBESEN, T. W., MIOSKOWSKI, C. Helical crystallization of proteins on carbon nanotubes: A first step towards the development of new biosensors., *Angew. Chem. Int. Ed.* **1999**, 38, 1912–1915.
- 91 BRADLEY, K., BRIMAN, M., STAR, A., GRÜNER, G. Charge transfer from adsorbed proteins., *Nano Lett.* **2004**, 4, 253–256.
- 92 WANG, S., HUMPHREYS, E. S., CHUNG, S.-Y., DELDUCCO, D. F., LUSTIG, S. R., WANG, H., PARKER, K. N., RIZZO, N. W., SUBRAMONEY, S., CHIANG, Y.-M., JAGOTA, A. Peptides with selective affinity for carbon nanotubes., *Nat. Mater.* **2003**, 2, 196–200.
- 93 BRADLEY, K., GABRIEL, J.-C. P., BRIMAN, M., STAR, A., GRÜNER, G. Charge transfer from ammonia physisorbed on nanotubes., *Phys. Rev. Lett.* **2003**, 91, 218 301-1–218 301-4.
- 94 WILSON-KUBALEK, E. M., BROWN, R. E., CELIA, H., MILLIGAN, R. A. Lipid nanotubes as substrates for helical crystallization of macromolecules., *Proc. Natl. Acad. Sci. U.S.A.* **1998**, 95, 8040–8045.
- 95 CHEN, R. J., CHOI, H. C., BANGSARUNTIP, S., YENILMEZ, E., TANG, X., WANG, Q., CHANG, Y. L., DAI, H. An investigation of the mechanisms of electronic sensing of protein adsorption on carbon nanotube devices., *J. Am. Chem. Soc.* **2004**, 126, 1563–1568.
- 96 BOUSSAAD, S., TAO, N. J., ZHANG, R., HOPSON, T., NAGAHARA, L. A. *In situ* detection of cytochrome c adsorption with single walled carbon nanotube device., *Chem. Comm.* **2003**, 1502–1503.
- 97 STAR, A., GABRIEL, J.-C. P., BRADLEY, K., GRÜNER, G. Electronic detection of specific protein binding using nanotube FET devices., *Nano Lett.* **2003**, 3, 459–463.
- 98 CHEN, R. J., BANGSARUNTIP, S., DROUVALAKIS, K. A., WONG SHI KAM, N., SHIM, M., LI, Y., KIM, W., UTZ, P. J., DAI, H. Noncovalent functionalization of carbon nanotubes for highly specific electronic biosensors., *Proc. Natl. Acad. Sci. U.S.A.* **2003**, 100, 4984–4989.
- 99 LI, H., NG, H. T., CASSELL, A., FAN, W., CHEN, H., YE, Q., KOEHNE, J., HAN, J., MEYAPPAN, M. Carbon nanotube nanoelectrode array for ultrasensitive DNA detection., *Nano Lett.* **2003**, 3, 597–602.
- 100 STAR, A., TU, E., NIEMANN, J., GABRIEL, J.-C. P., JOINER, C. S., VALCKE, C. Label-free detection of DNA hybridization using carbon nanotube field-effect transistors., *Proc. Natl. Acad. Sci. U.S.A.* **2006**, 103, 921–926.
- 101 LIMDI, J. K., CRAMPTON, J. R. Hereditary haemochromatosis., *Q. J. Med.* **2004**, 97, 315–324.
- 102 FRANCHINI, M., VENERI, D. Recent advances in hereditary hemochromatosis., *Ann. Hematol.* **2005**, 84, 347–352.
- 103 TANG, X., BANGSARUNTIP, S., NAKAYAMA, N., YENILMEZ, E., CHANG, Y.-I., WANG, Q. Carbon nanotube DNA sensor and sensing mechanism., *Nano Lett.* **2006**, 6, 1632–1636.
- 104 MAEHASHI, K., MATSUMOTO, K., KERMAN, K., TAKAMURA, Y., TAMIYA, E. Ultrasensitive detection of DNA hybridization using carbon nanotube field-effect transistors., *Jpn. J. Appl. Phys.* **2004**, 43, L 1558–L 1560.
- 105 STAR, A., JOSHI, V., HAN, T. R., ALTOE, V. P., GRÜNER, G., STODDART, J. F. Electronic detection of the enzymatic degradation of starch., *Org. Lett.* **2004**, 6, 2089–2092.
- 106 KONG, J., DAI, H. Full and modulated chemical gating of individual carbon nanotubes by organic amine compounds., *J. Phys. Chem B* **2001**, 105, 2890–2893.
- 107 SHIM, M., JAVEY, A., KAM, N. W. S., DAI, H. Polymer functionalization for air-stable n-type carbon nanotube field-effect transistors., *J. Am. Chem. Soc.* **2001**, 123, 11 512–11 513.
- 108 BESTEMAN, K., LEE, J. O., WIERTZ, F. G. M., HEERING, H. A., DEKKER, C. Enzyme-coated carbon nanotubes as single-molecule biosensors., *Nano Lett.* **2003**, 3, 727–730.